Negative Feedback Regulation in Hierarchically Organized Tissues: Exploring the Dynamics of Tissue Regeneration and the Role of Feedback Escape in Tumor Development

Ignacio A. Rodriguez-Brenes, Natalia L. Komarova, and Dominik Wodarz

Abstract Hierarchically organized tissues are tightly regulated to maintain homeostasis under normal conditions and promote the rapid regeneration after injury. Negative feedback from the tissue itself plays an important role in establishing this control. In particular differentiated cells emit signals that down-regulate cell division and inhibit stem cell self-renewal. The mathematical analysis of how these two feedback mechanisms affect tissue regeneration and stability can provide important insights into the dynamics of tissue regulation. This topic is also important for the study of carcinogenesis, given that cancer development requires an escape from feedback control. Here we discuss various aspects of tissue regulation and the phenotypic evolutionary pathways that lead to escape from these feedback mechanisms. Furthermore, we discuss the various tumor growth patterns that arise through different feedback inactivations. Finally, by examining published clinical data we propose that the majority of tumor growth patterns found in the literature can be classified into five categories, which by themselves could reflect the different evolutionary events that drive tumor progression in different types of stem-cell-driven cancers.

1 Introduction

In cell lineages tissue development, maintenance and regeneration are highly regulated. In healthy tissue control loops ensure that the number of cells are kept at appropriate levels, precluding the appearance of abnormal cell growth and promoting the efficient regeneration after an injury [17,47]. Two types of feedbacks

I.A. Rodriguez-Brenes • N.L. Komarova
Department of Mathematics, University of California, Irvine, CA 92697, USA
e-mail: iarodrig@uci.edu; komarova@uci.edu

D. Wodarz (✉)
Department of Ecology and Evolution, University of California, Irvine, CA 92697, USA
e-mail: dwodarz@uci.edu

A. Eladdadi et al. (eds.), *Mathematical Models of Tumor-Immune System Dynamics*, Springer Proceedings in Mathematics & Statistics 107,
DOI 10.1007/978-1-4939-1793-8_8

have been identified: long-range and short-range [4]. The long-range feedbacks respond to the loss of mature cells during an injury, while the short-range feedbacks act in an autocrine fashion in stem cells [3, 6]. In this chapter we will focus on long-range feedbacks. In particular, two types of feedback loops have been suggested to be crucial: Differentiated cells secrete factors that inhibit the division of stem cells. In addition, differentiated cells secrete factors that suppress self renewal of stem cells and instead promote differentiation of the stem cells [26, 33, 60]. This stops the expansion of the stem cell population and leads to cell death through terminal differentiation, thus stopping tissue growth. Negative feedback regulators have been identified in a large number of tissues including muscle, liver, bone, hair, and the nervous and hematopoietic systems [13, 14, 33, 55, 61].

In this chapter we present a mathematical model, which includes feedback regulation in both the division rate and the self-renewal probability of stem cells. We find that the feedback on the self-renewal probability of stem cells is by itself sufficient to establish control. However, if feedback on the division rate is absent, tissue regeneration may lead to significant damped oscillations in the path back to recovery, which, in the worst case scenario, could even lead to the stochastic extinction of the cell population. We find that this oscillatory behavior is more pronounced when the number of stem cell is only a small fraction of the cell population. In general we find a trade-off between requiring a small equilibrium fraction of stem cells while avoiding oscillations and the speed at which the system is able to recover from a perturbation. Spatial interactions and the addition of feedback inhibition on the cell division rate reduce the amplitude of oscillations and contribute to the robustness of the system. In addition, feedback inhibition on the division rate also increases the speed of regeneration.

This discussion falls within the context of ongoing mathematical research on the areas of tissue regulation and cancer development. The mathematical modeling of cancer stem cells and cell compartments has lead to significant biological insights (see e.g. [15, 41, 54, 58]). In particular numerous mathematical models explore hematopoiesis and different types of blood cancers [1, 5, 12]. Negative feedback regulation through control loops has been explored in various tissues including the olfactory epithelium, hematopoietic system, and intestinal crypts [7, 23, 26].

Evidence suggests that tumors retain basic architectural components characteristic of healthy tissue, containing so called ‘cancer stem cells’ or ‘cancer initiating cells’ that maintain the disease, which leads to the concept of stem-cell-driven tumors [11]. Carcinogenesis is a complex process, in which different aspects such as angiogenesis, nutrient availability, metabolic processes, interactions with the microenvironment, and immune responses all influence how the tumor grows and evolves [57]. Despite this great complexity and heterogeneity in the mechanism of tumor formation, it is reasonable to postulate that escape from feedback regulation must be a key ingredient in the formation of any stem-cell-driven tumor.

In this chapter we discuss a computational evolutionary model which suggests that full escape from feedback inhibition can only proceed through a unique sequence of phenotypic transitions. Furthermore, we propose that these dynamics are a common feature amongst the majority of stem-cell-driven tumors, even if

the nature and number of the mutational events required to achieve an escape from feedback regulation are certainly tissue specific. We find that the specific pathways that lead to uncontrolled proliferation, together with the composition of the tissue (solid or non-solid), determine the tumor growth pattern that will take place. According to our models these patterns can be classified into five different categories, which is supported by data fitting and an extensive search of the tumor growth data reported in the literature.

2 Model of Feedback Regulated Tissue Homeostasis

In order to examine the evolutionary dynamics of feedback loss, we will first discuss a computational model that describes feedback-regulated tissue homeostasis, and then add mutational processes to this model. We consider two types of cells: stem cells that are characterized by their ability to differentiate and self renew through cell division, and differentiated cells that do not divide (this includes all cells that do not have a full capacity to self-renew, for example transit amplifying cells). When a stem cell divides it may produce either two stem cells with probability p, or two differentiated daughter cells with probability $1 - p$ (including asymmetric stem cell divisions leads to an equivalent mathematical formulation and does not alter any of the results). In accordance with experimental data, we assume that differentiated cells produce two regulatory factors: one reduces the probability of stem cell self renewal and promotes differentiation; the other reduces the rate of cell division. Thus, a high number of differentiated cells reduces proliferation and increases the rate of differentiation, which eventually leads to a reduction of the overall cell population through terminal differentiation. If we call the division rate of stem cells v and the death rate of differentiated cells d the model is represented schematically by Fig. 1a.

The system of ordinary differential equations (1) describes the model's behavior, where S is the number of stem cells and D the number of differentiated cells. The self renewal probability of stem cells $p(D)$ and the division rate $v(D)$ are treated as general functions that depend on the number of differentiated cells D. This ensures that results are not dependent on the particular mathematical expressions used to describe feedback inhibition. The functions obey the following constraints. First we require that the self renewal probability as well as the division rate of stem cells are differentiable decreasing functions of the number of differentiated cells D. Also, it is assumed that $0.5 < p(0) \leq 1$, i.e., the maximum probability of self renewal, $p(0)$, has to be greater than 0.5 (otherwise the stem cell population will go extinct). Finally, we require that the feedback functions go to zero as the number of differentiated cells grow without bound.

$$\begin{aligned} \dot{S} &= (2p(D) - 1)\, v(D)\, S \\ \dot{D} &= 2(1 - p(D))\, v(D)\, S - d\, D \end{aligned} \tag{1}$$

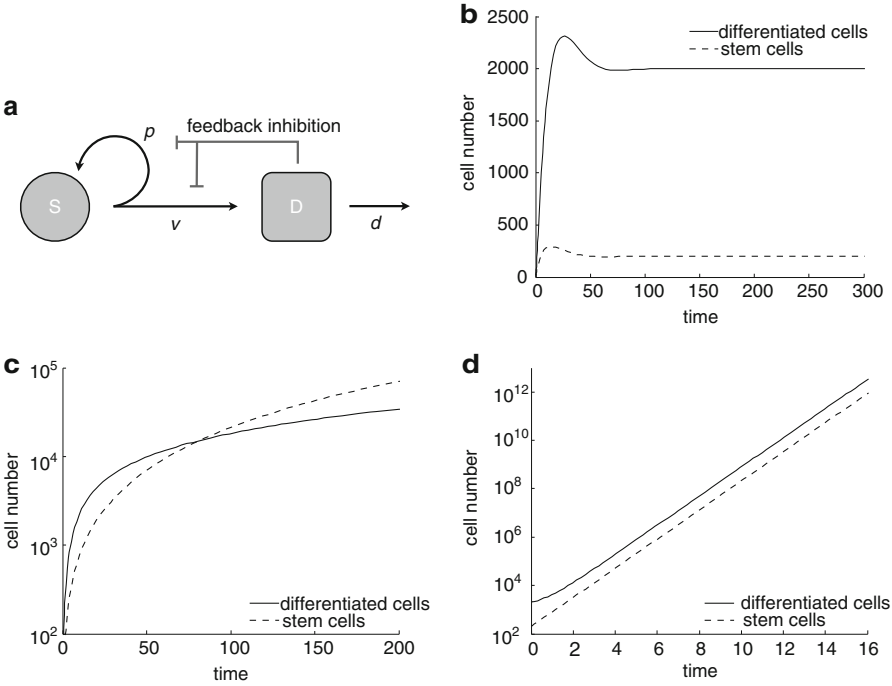

Fig. 1 Feedback-regulated tissue homeostasis and cell growth properties. (**a**) Stem cells divide at a rate v producing either two stem cells with probability p or two differentiated cells with probability $(1-p)$. Differentiated cells die at a rate d and produce factors that promote cell differentiation and inhibit division in stem cells. (**b**) If the feedback loops satisfy specific conditions (discussed in the text) the system has a unique equilibrium point that is independent of the initial conditions and is asymptotically stable. (**c**) *Inhibited growth*. If only differentiation feedback is lost, the population of stem cells and differentiated cells grows without bound at a slower than exponential rate. (**d**) *Uninhibited growth*. If both feedbacks are lost stem cells and differentiated cells grow at a rate dominated by the same exponential. Time is expressed in units of $\ln 2/v(\hat{D})$, the expect duration of one cell cycle at equilibrium. Functional forms used to produce the figure: $p(D) = p_0/(1+gD)$ and $v(D) = v_0/(1+hD)$; $p_0 = 0.6, v_0 = 6.93, d = 6.93 \times 10^{-2}, h = 4.5 \times 10^{-3}, g = 10^{-4}$

System (1) has exactly one nonzero equilibrium point $(\hat{S}, \hat{D})$, defined by the conditions $p(\hat{D}) = 0.5$ and $\hat{S} = d\,\hat{D}/v(\hat{D})$. We proved in [38] that this equilibrium point is asymptotically stable if and onlyif $-p'(\hat{D}) < 1/(2\hat{D})$ (Fig. 1b). Two examples of families of functions that satisfy this condition are given by (2). There are no additional requirements imposed on the function $v(D)$.

$$\begin{aligned} p(D) &= p_0/(1 + g\log(1+D)) \;, 0 < g < 1 \\ p(D) &= p_0/(1 + gD^m) \qquad\quad , 0 < g,\ 0 < m \ (\text{for } m > 1,\ p_0 < \tfrac{m}{2(m-1)}) \end{aligned} \tag{2}$$

3 Feedback Loss and Cell Growth Properties

In this section we will use the model of tissue homeostasis to study the evolutionary dynamics of feedback escape and the consequent emergence of uncontrolled cellular growth. In the model abnormal cell growth occurs when the feedback mechanisms that control the size of the cell population fail. Failures in each of the two feedback mechanisms produce different results. If feedback on the division rate is completely lost, the system remains stable, the steady state number of differentiated cells does not change, and the steady number of stem cells decreases from $d\hat{D}/v(\hat{D})$ to $d\hat{D}/v(0)$. If on the other hand the differentiation feedback is completely lost, we find that the division rate feedback by itself is incapable of controlling cell growth: both the number of stem cells and differentiated cells grow without bound (Fig. 1c). These observations point to the differentiation feedback as the more fundamental of the two control mechanisms. However, even though feedback on the division rate is by itself incapable of stopping abnormal growth, it does play a critical role by significantly slowing down the rate of cell proliferation. If feedback inhibition on stem cell self-renewal is lost, but the feedback on the division rate is still intact, then the population dynamics are characterized by a relatively slow sub-exponential increase of the numbers that we called "inhibited growth" (Fig. 1c). When both feedbacks are lost the growth of the cell population occurs at a faster exponential rate, which we call "uninhibited growth" (Fig. 1d).

There is another distinctive difference between inhibited and uninhibited growth. When uninhibited growth takes place, the ratio of stem cells to differentiated cells in the population converges to a fixed number $((2p_0 - 1)v_0 + d)/(2(1 - p_0)v_0)$. With inhibited growth, we find that this ratio cannot converge. More precisely, the ratio of stem cells to differentiated cells goes to infinity (Fig. 1c). Thus, inhibited tumor growth is relatively slow and characterized by a predominance of stem cells in the cell population at late stages of its development; while uninhibited tumor growth is faster and is characterized by a constant ratio of stem cells to differentiated cells.

4 Mutations and the Evolutionary Dynamics of Feedback Loss

Here we investigate the evolutionary dynamics of cells that carry mutations responsible for corrupted feedback mechanisms. Such cells must emerge from healthy cells and have a growth advantage in order to initiate tumor growth. Mutations can corrupt either the division feedback or the differentiation feedback. In each case, mutations can lead to failures in the production of feedback signals by differentiated cells, or to failures in the response to these signals by stem cells. Hereafter we will call the wild type stem and differentiated cells S and D, and the mutant stem cells and differentiated cells S_m and D_m. We assume that a mutation occurs in one or a small group of stem cells, and that the daughters of the mutant stem cells carry

the same mutations as their parent. We will denote mutations that cause a failure in production of feedback signals by differentiated cells with the prefix D; and those that lead to a failure of response by stem cells to these signals with the prefix S. Mutations that affect cell differentiation will carry the suffix diff- and those that affect the division rate the suffix div-. Note that when we refer to a mutation event that inactivates certain feedback processes, we do not imply that a single mutation is sufficient to achieve this. Indeed, an accumulation of mutations is likely necessary. In the computational model, what we study are the transitions from one phenotype to another; we do not explicitly take into account the number of genetic steps required to attain a particular phenotype, which are certainly specific to the tissue in question.

We consider four types of mutations:

- Stem cells with mutation Ddiff- generate differentiated cells that do not produce the differentiation-promoting factor (described by system (3)).
- Stem cells with mutation Sdiff- do not respond to the differentiation-promoting factor (described by system (4)).
- Stem cells with mutation Ddiv- generate differentiated cells that do not produce the division-inhibiting factor (described by system (5)).
- Stem cells with mutation Sdiv- do not respond to the division-inhibiting factor (described by system (6)).

$$\begin{aligned}
\dot{S} &= (2p(D)-1)\,v(D+D_m)\,S \\
\dot{D} &= 2(1-p(D))\,v(D+D_m)\,S - dD \\
\dot{S}_m &= (2p(D)-1)\,v(D+D_m)\,S_m \\
\dot{D}_m &= 2(1-p(D))\,v(D+D_m)\,S_m - dD_m
\end{aligned} \tag{3}$$

$$\begin{aligned}
\dot{S} &= (2p(D)-1)\,v(D)\,S \\
\dot{D} &= 2(1-p(D))\,v(D)\,S + (2p_0-1)\,v(D)\,S_m - dD \\
\dot{S}_m &= (2p_0-1)\,v(D)\,S_m
\end{aligned} \tag{4}$$

$$\begin{aligned}
\dot{S} &= (2p(D+D_m)-1)\,v(D)\,S \\
\dot{D} &= 2(1-p(D+D_m))\,v(D)\,S - dD \\
\dot{S}_m &= (2p(D+D_m)-1)\,v(D)\,S_m \\
\dot{D}_m &= 2(1-p(D+D_m))\,v(D)\,S_m - dD_m
\end{aligned} \tag{5}$$

$$\begin{aligned}
\dot{S} &= (2p(D)-1)\,v(D)\,S \\
\dot{D} &= 2(1-p(D))\,v(D)\,S + (2p(D)-1)\,v_0\,S_m - dD \\
\dot{S}_m &= (2p(D)-1)\,v_0\,S_m
\end{aligned} \tag{6}$$

We now summarize the main findings in [38]. Mutations that induce a lack of production by differentiated cells of signals that control cell division and differentiation (Ddiv- and Ddiff-, respectively) do not confer a competitive advantage to cells that carry them. This absence of competitive advantage is intuitively explained

by the fact that at any time t the feedback signals are the same for the wild type and mutant stem cells (Eqs. (3) and (5)). If these mutations arise in a very small number of cells, as one should expect from a random mutation, the steady state number of mutant stem cells would remain at a negligible level (Fig. 2a). Moreover, in a stochastic formulation the probability that this species goes extinct is very high. A similar result applies to the mutation inducing a lack of response by stem cells to the division feedback signals Sdiv-. If the system is near equilibrium when the mutation emerges in one cell, the steady state percentage of mutant stem cells will be very small. In practice this means that these three mutations would, in all likelihood, disappear from the cell population. An entirely different scenario occurs if cells acquire a mutation that leads to a loss of response by stem cells to signals that control differentiation Sdiff-. This mutation does confer a competitive advantage to cells that carry it: eventually the mutant stem cells will take over the entire stem cell population and the total number of cells grows without bound (Fig. 2b,d).

Another possibility is that a mutation confers only a partial loss of response to signals that control cell differentiation (denoted by Sdiff-/partial). This scenario is modeled by system (7) where $\tilde{p}(D) \geq p(D)$. In this case the mutation leads to a finite increase in the number of both mutant stem cells and differentiated cells, which results in a sigmoidal growth pattern (Fig. 2c). The size of this increase depends on how diminished the response to the differentiation-promoting factors is. The wild type stem cells go extinct and the ratio of stem cells to differentiated cells does not change.

$$\begin{aligned} \dot{S} &= (2p(D) - 1)\, v(D)\, S \\ \dot{D} &= 2(\,1 - p(D)\,)\, v(D)\, S + 2(1 - \tilde{p}(D))v(D)\, S_m - d\, D \\ \dot{S}_m &= (2\tilde{p}(D) - 1)\, v(D)\, S_m \end{aligned} \tag{7}$$

According to our analysis, the first step towards uncontrolled proliferation must be the loss of stem cell response to the differentiation feedback. We now want to investigate what happens to the cell population if a subsequent mutation occurs in a cell that carries mutation Sdiff-. We find that two types of double mutants, Sdiff-/Ddiff- and Sdiff-/Ddiv-, do not have a competitive advantage to single mutants Sdiff-. If the additional mutation occurs in a single cell, the number of stem cells with a double mutation grows (like the rest of the cell population), but it remains as a very small percentage of the stem cell population. As a result the growth dynamics of the entire cell population do not change in any significant way. A different scenario occurs if the second mutation is Sdiv-. In this case the number of double mutants Sdiff-/Sdiv- grows at an exponential rate while single mutants would continue to growth at a much slower sub-exponential pace. As a result the number of single mutants would eventually become a negligible percentage of the total number of cells and the entire cell population would appear to grow at an exponential rate.

Finally, there is the possibility that a mutation produces only a partial loss in the ability to respond to feedback factors that control the rate of cell division (denoted

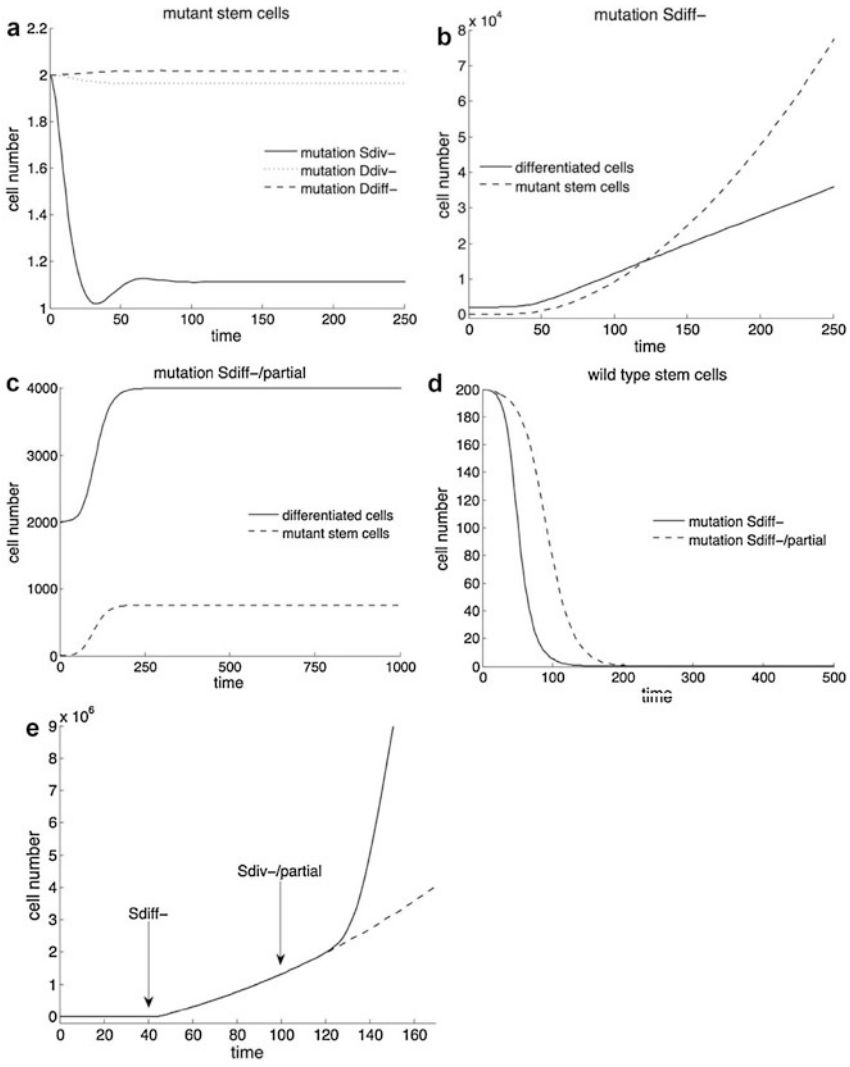

Fig. 2 Evolutionary dynamics of feedback loss. The simulations begin at equilibrium with two stem cells carrying the specified mutation. (**a**) For populations near equilibrium, mutations Sdiv-, Ddiv- and Ddiff- do not confer any competitive advantages over their wild type counterparts. If the mutation arises in a small number of cells, the steady state number of mutant stem cells will be negligible. (**b**) Mutation Sdiff- results in unlimited growth in the number of mutant stem cells and differentiated cells. (**c**) Mutation Sdiff-/partial produces a finite increase in both the number of mutant stem cells and differentiated cells. (**d**) Mutations Sdiff- and Sdiff-/partial result in the extinction of the wild type stem cell population. (**e**) In a cell population that carries mutation Sdiff- (*dashed line*) the appearance of mutation Sdiv-/partial produces an acceleration in the growth rate of the tumor size (*solid line*). (**f**) Tumor progression towards uninhibited growth follows a unique sequence of feedback inactivations: first mutation Sdiff- must occur, followed by mutation Sdiv-. Simulations use the functional forms and parameters of Fig. 1. In panel 2C, $\tilde{p}(D) = 0.1p(D)$; in 2E, $\tilde{\nu}(D) = 0.05p(D)$

by Sdiv-/partial). If this type of mutation emerges in a population of wild type cells the steady state number of mutants will be negligible and invasion is not possible. However, if the mutation appears in a population of cells that has completely lost feedback on differentiation (mutation Sdiff-), this diminished response to the division rate factors will accelerates the rate of tumor growth (Fig. 2e).

This analysis suggests that full escape from feedback-regulated tissue homeostasis can only occur via a unique sequence of phenotypic transitions that we propose to be common among stem-cell-driven tumors, even if the nature and number of mutational events required to achieve this are certainly tissue specific. First, a mutation must occur that inactivates the ability of stem cells to respond to differentiation feedback factors. In a second step, a mutation has to inactivate the ability of stem cells to respond to division feedback factors. Note that the order in which these mutation types occur is crucial. In terms of growth dynamics, this would lead to an initial slow (inhibited) growth, followed by a fast (uninhibited) growth phase. However, it is important to mention that by the time a tumor is detected, both sets of mutations might have already occurred and thus the transition between both growth phases might not be clinically observed.

5 Evolutionary Dynamics in a Spatial Model

The analysis performed so far uses ordinary differential equations that assume perfect mixing of cells (i.e., no spatial structure) and does not take into account any stochastic effects. This can be a good description for non-solid tumor growth, which allows us to gain a thorough analytical understanding of the system. Many tumors, however, exhibit three-dimensional spatial structure. In this section, we investigate the evolutionary dynamics of feedback loss in a spatial stochastic model.

To construct the spatial model we assume that cells are restricted to a three-dimensional rectangular lattice, such that a lattice point can host at most one cell at any time. As before, stem cells divide producing either two stem cells or two differentiated cells. A cell is capable of cell division only if there is a free lattice point adjacent to it. If a cell division takes place, then one offspring remains in the position occupied by the parent cell and the other occupies a position next to it, which is chosen randomly from the free adjacent lattice points. The simulations are based on the stochastic simulation algorithm [20], where the probabilities of cell division, differentiation, and death correspond to our previous non-spatial mass action model. More precisely let S and D be the number of differentiated cells at a given time t. Let $F \leq S$ be the number of stem cells that are able to divide and α, β and γ be defined by: $\alpha = dD$, $\beta = Fv(D)$, and $\gamma = \alpha + \beta$. To implement the algorithm, set the time of the next reaction to $t' = t - 1/\gamma \log(r)$, where r is a random number uniformly distributed in $[0, 1)$. Then choose the type of reaction that occurs. The next reaction will be either cell death with a probability α/γ, or cell division with a probability β/γ. If the next reaction is cell death, every differentiated cell has the same probability of being chosen; if it is cell division; every stem cell

that is able to divide has the same probability of being selected. Finally, if cell division occurs, the probability that the cell divides into two stem cells is $p(D)$, and the probability that it divides into two differentiated cells is $1 - p(D)$; the place where one of the offspring will reside is chosen at random, with each available adjacent position having an equal probability of hosting one of the daughter cells.

In the spatial stochastic model we find the same basic dynamics of feedback escape (Fig. 3). Again, we observe uninhibited tumor growth if both feedback loops are broken, and inhibited growth when only the differentiation feedback loop is lost. In agreement with the non-spatial model, the percentage of stem cells in the cell population increases progressively with inhibited growth (Fig. 3b), while it converges to a fixed percentage for uninhibited growth. However, in contrast to the non-spatial situation, the tumor growth rates are slower. Uninhibited growth is now

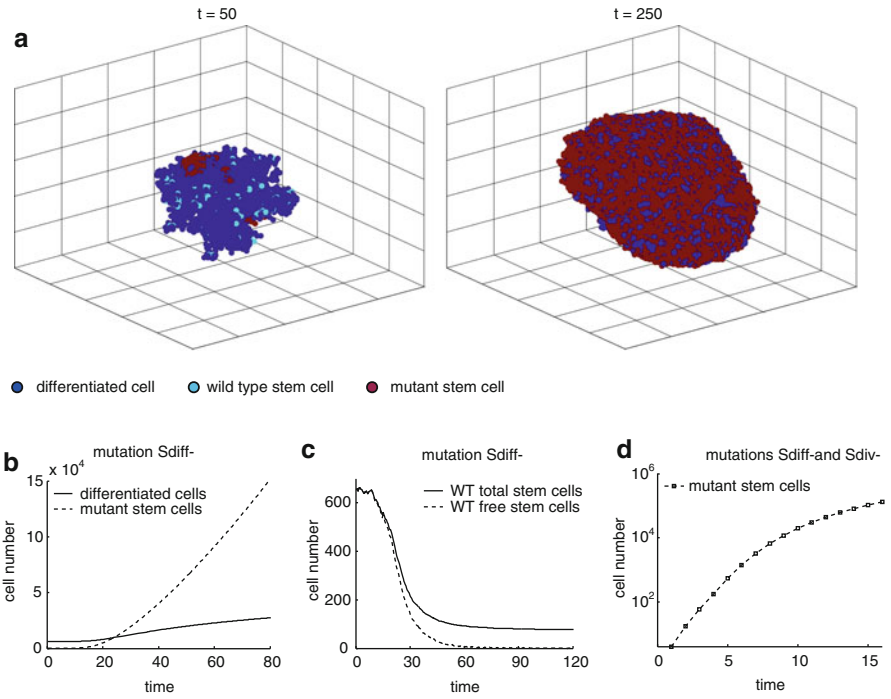

Fig. 3 Spatial model. (**a**) Spatial arrangement of the cell population at two different times. The simulation begins with a tissue at near equilibrium with two stem cells randomly selected to carry mutation Sdiff- at time $t = 0$. (**b**) The appearance of mutation Sdiff- results in the unlimited growth of the mutant stem cell and differentiated cell populations. (**c**) The number of wild type stem cells decreases. Note that a small number of stem cells that are trapped—and thus unable do divide—lingers in the population for a long time. The number of wild type stem cells, however, becomes a negligible percentage of the entire cell population (see text for discussion). (**d**) Cell population with stem cells carrying mutations Sdiff- and Sdiv-. Cell growth is much faster than if only mutation Sdiff- is present; but, unlike the non-spatial model, the growth is not exponential

cubic (not exponential) and inhibited growth sub-cubic (Fig. 3d). This is explained by the fact that in the 3D model the number of stem cells that are able to divide (free cells) is smaller than the total number of stem cells. We also find that full feedback escape can only occur through the same unique sequence of phenotypic transitions. The only mutation that by itself confers a fitness advantage is *S*diff-. The transition from inhibited to uninhibited growth occurs when an *S*diff- mutant acquires the additional mutation *S*div-.

Finally, we note that in the spatial model, when the number mutant stem cells increases the number of wild type stem cells goes down, but a small number of wild type stem cells might persist in the population for a long period of time (Fig. 3c). Indeed, as the overall cell population grows a number of wild type stem cells might get spatially trapped by surrounding cells leaving them no space available to divide. (Fig. 3a). As the cell population grows, however, the number of wild type stem cells becomes a negligible part of the cell population.

Table 1 Fitting parameters in Fig. 5. The functional forms used are $p(D) = p_0/(1 + g\sqrt{D})$ and $v(D) = v_0/(1 + h\sqrt{D})$. For details about the fitting procedure see the methods section in [38]

Figure	p_0	v_0	d	h	g
5A	0.71	0.31 Hours^{-1}	0.736 Hour^{-1}	2.22×10^{-3}	0
5B	0.55	295 Hours^{-1}	126 Hours^{-1}	3.67×10^{-3}	0
5C	0.62	6.29 Days^{-1}	0.251 Days^{-1}	0	0
5D	0.68	1.46 Days^{-1}	0.146 Days^{-1}	0	0
5E	0.67	2.91 Days^{-1}	5.93 Days^{-1}	0	1.74×10^{-4}

6 Predicted Versus Experimentally Observed Growth Patterns

The models analyzed here predict the occurrence of five basic growth patterns, which can be categorized as: exponential, surface, atypical, sigmoidal and multi-step [40]. The first two patterns correspond to uninhibited growth: exponential growth in non-spatial tumors and surface (cubic) growth in spatial tumors. In this categorization both types of inhibited growth (sub-cubic in spatial tumors and sub-exponential in non-spatial tumors) are grouped together under the name of atypical tumor growth. Multi-step growth occurs when a sequence of mutations of type *S*diff-/partial progressively erode the stem cells' ability to respond to feedback signals that promote differentiation. Figure 4 summarizes the different types of mutations and the evolutionary pathways that produce each of these growth patterns.

In the next subsection we will provide references of published tumor growth data for each of the growth patterns discussed. We will also provide data fits for our models. Our modeling approach assumes general functions describing the feedbacks $p(D)$ and $v(D)$; however, data fitting algorithms require us to choose specific functional forms. To produce these fits we use Hill functions to model feedback inhibition (8). Hill functions are widely used to describe ligand–receptor interactions, which make them natural choices to model the actions of secreted feedback factors [2]. Moreover, they have been used extensively to model the specific phenomena of tissue regulation in cell lineage models [7, 10, 26, 30, 42, 62]. The precise data fitting procedures can be found in [38].

$$p(D) = p_0/(1 + gD^n), \quad v(D) = v_0/(1 + hD^m) \tag{8}$$

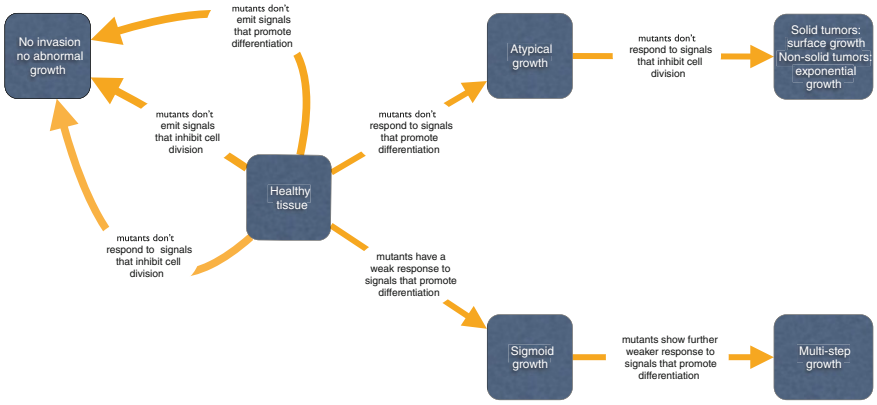

Fig. 4 Schematic representation of the possible phenotypic mutations and their effects on the cell population. According to the model of feedback regulation different evolutionary pathways produce the various tumor growth patterns observed in the literature (See text for discussion)

6.1 Exponential Growth

In our framework this type of growth takes place when feedback on differentiation and feedback on cell division is lost in non-spatial tissues. The growth pattern is produced by the emergence of double mutants Sdiff-/Sdiv-.

Experimentally evidence for exponential tumor growth has been reported in various types of human and murine leukemias [46, 50, 52]. Figure 5c presents In vivo

growth data of L1210 cells [46], a mouse lymphocytic leukemia, which exhibits exponential dynamics representative of an uninhibited growth pattern in a non-spatial setting. The best fit resulted in a value of $g = 0$ and $h = 0$, the case when both feedbacks are lost.

6.2 Surface Growth

In our framework this type of growth takes place when feedback on differentiation and feedback on cell division is lost in spatial tissues. The growth pattern is produced by the emergence of double mutants Sdiff-/Sdiv-. Intuitively this growth pattern takes place when the active growth of a solid tumor is limited to a thin surface layer of cells located near the tumor's boundary.

Experimental evidence for surface tumor growth has been reported in rat sarcomas [24], multicellular tumor spheroids [18, 19], in vitro colonies of various immortalized cancer cell lines [8], and glioblastomas [29]. In Fig. 5d we plot in vitro data from multicellular tumor spheroids of EMT6/Ro cells [19], a mouse mammary tumor. The data shows approximately cubic surface growth (as seen by plotting the cube root of the cell numbers). The best fit of the model occurred when both feedbacks were lost ($g = 0$, $h = 0$).

6.3 Atypical Growth

In our framework this type of growth takes place when feedback on differentiation is lost, but feedback on the division rate is still operating. The growth pattern is produced by the emergence of single mutants Sdiff-.

Experimental evidence for atypical tumor growth has been reported in breast cancer [22], ovarian carcinoma [48], Ehrlich's ascites tumor [25] and murine leukemia [49]. In Fig. 5a we plot data from Ehrlich's ascites tumor [25] growing in vivo. This tumor, which originated spontaneously as a breast carcinoma in a mouse, grows in ascitic form, i.e., cells mix well. The data shows sub-exponential growth with no saturation, suggesting an inhibited growth pattern. The best fit resulted in a value of $g = 0$ and $h > 0$, a scenario where there is a complete loss of differentiation feedback, but feedback on the division rate is still present. In Fig. 5b we fitted the spatial model to data from A2780 human ovarian carcinoma [48] (a solid tumor) growing in mice. The data shows sub-cubic behavior with a power law of 2.17 and no saturation, consistent with a description of inhibited growth in a spatial setting. With this behavior in mind we fitted the data assuming that feedback on the division rate was still present, but feedback on differentiation had been lost. The main frame shows a projection of the model using the function $y = ax^b$; in the inset the results from the model are plotted together with this function. Simulations were not carried further due to computational constraints.

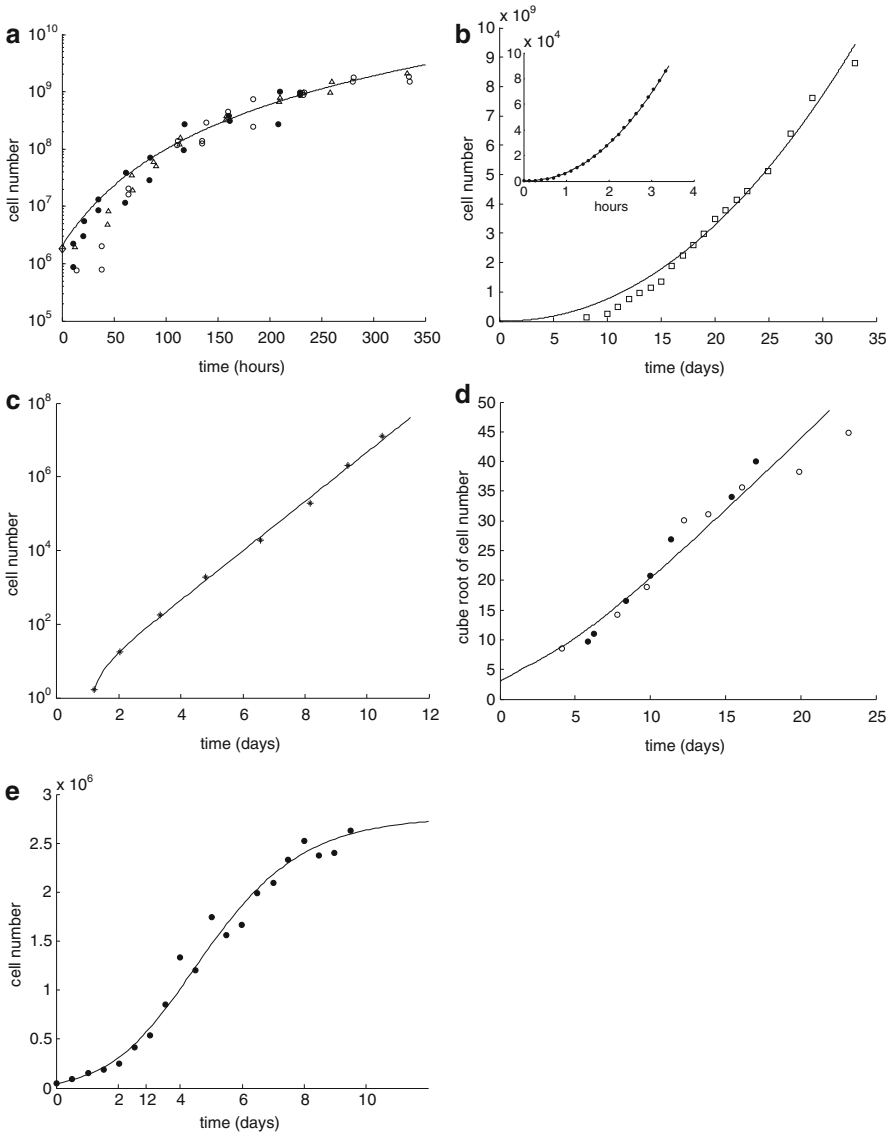

Fig. 5 Experimentally observed growth patterns. (**a**) Atypical pattern. *Inhibited* growth in the non-spatial model. Ehrlich ascites tumor [25] (three experiments shown: •, △, ∘). (**b**) Atypical pattern. *Inhibited* growth in the spatial model. Main frame: (□) A2780 human ovarian carcinoma [48] and projection of the model (*solid line*). *Inset*: Simulation results (•) and projection using the functional form $y = ax^b$. (**c**) Exponential pattern. *Uninhibited* growth in the non-spatial model. (∗) L1210 a mouse lymphocytic leukemia [46]. (**d**) Surface pattern. *Uninhibited* growth in the spatial model. Multicellular tumor spheroids of EMT6/Ro cells [19], a mouse mammary tumor (two experiments shown: ∘, •). (**e**) Sigmoidal pattern. Example in non-spatial tumor. (•) Jurkat T cell human leukemia [37]. In all the plots the simulations are shown in *solid lines*; those corresponding to the spatial model represent the average of 24 runs. For parameters see Table 1

6.4 Sigmoidal Growth

In our framework this type of growth takes place when feedback on differentiation is only partially lost. The growth pattern is produced by the emergence of single mutants of type Sdiff-/partial.

Experimental evidence for sigmoidal tumor growth has been reported for a large number of tumors (see e.g. [21]), which include breast cancer [51, 56], multiple types of rodent tumors [9, 25], and human leukemia [37]. Figure 5e plots data of Jurkat cells [37], originating from a T cell human leukemia. The best fit resulted in a value of $g > 0$, a case where the differentiation feedback mechanism is only partially broken.

6.5 Multi-Step Growth

In our framework this type of growth takes place when a sequence of mutations progressively erode the stem cells' ability to respond to feedback signals that promote differentiation. The growth pattern is produced by sequential acquisitions of the mutations of the type Sdiff-/partial.

This type of growth pattern is at least partially backed by the theory of multistage carcinogenesis. According to this theory, cancer is primarily a genetic disease that requires cells to accumulate sequentially several random mutations and epigenetic changes [34, 35]. Experimental evidence for multi-step tumor growth has been reported in multiple mouse mammary tumors [53] and several types of human sarcomas and carcinomas [36].

7 Dynamics of Tissue Regulation

As we saw in the previous sections tumor initiation requires an escape from the control mechanisms that maintain tissue homeostasis. It is fundamental then to understand the regulatory mechanisms themselves and how their dynamics are shaped by two objectives: promoting the rapid regeneration after an injury and maintaining tissue homeostasis under normal conditions.

Let us again focus our attention on the regulation of the rates of stem cell division and self-renewal by negative feedback factors and go back to the analysis of system (1). First, as we recall that the equilibrium number of stem cells $\hat{S}$ and differentiated cells $\hat{D}$ is characterized by the conditions $p(\hat{D}) = 1/2$ and $\hat{S} = d\,\hat{D}/v(\hat{D})$. Hence, the equilibrium number of differentiated cells $\hat{D}$ depends only on the self-renewal probability $p(D)$, and the equilibrium fraction of stem cells $\hat{S}/(\hat{S} + \hat{D})$ on the ratio $d/v(\hat{D})$. To understand the recovery of the system after a

perturbation we look at the eigenvalues of the Jacobian matrix evaluated at $(\hat{S}, \hat{D})$. If we write $b = (2p'(\hat{D})\hat{D} + 1)$ and $\hat{v} = v(\hat{D})$, the eigenvalues are:

$$\lambda_1, \lambda_2 = \frac{-db \pm \sqrt{d^2b^2 + 4d(b-1)\hat{v}}}{2} \tag{9}$$

From this last equation it follows that the equilibrium values are asymptotically stable if and only if $b > 0$. Conversely if $b < 0$, the equilibrium is unstable. If $b = 0$ a Hopf bifurcation might be possible, but this would depend on the specific choice of the regulation functions $v(D)$ and $p(D)$.

In most tissues the number of stem cells makes up only a small fraction of the entire cell population [57]. It is important then to understand how this requirement affects the cell dynamics of the regulatory system. In particular we will find that the equilibrium fraction of stem cells is related to the possibility of oscillatory behavior after an injury.

To avoid oscillation near the equilibrium point we need the discriminant Δ in (9) to be non-negative. As we mention earlier the fraction of stem cells is completely determined by the ratio $\varepsilon = d/\hat{v}$: the smaller ε the smaller the fraction of stem cells. We prove in [39] that if $\Delta \geq 0$, then:

$$\lim_{\varepsilon \to 0} \lambda_1, \lambda_2 = -d, 0 \tag{10}$$

Now, if the absolute value of one of the eigenvalues is very small, then the dynamics of the system are characterized by rapid approach to a slow manifold, followed by a very slow approach toward equilibrium. Hence, we find a trade-off between requiring a small equilibrium fraction of stem cells (ε small) while avoiding oscillations and the speed at which the system is able to recover from a perturbation (influenced by the magnitude of the eigenvalues).

We find then that the existence of a stable nontrivial steady state is independent of feedback inhibition on the division rate. Moreover, for a fixed equilibrium division rate $\hat{v}$ the steady state population sizes are independent on the actual function $v(D)$. The role of feedback on the division rate in the system lies instead in increasing the speed at which the system recovers from a perturbation and reducing the amplitude of oscillations if they happen to occur.

To illustrate these dynamics we perform simulations using Hill equations (8) to model the feedback functions $p(D)$ and $v(D)$. Figure 6a,b track the trajectory of a cell population that only has feedback on stem cell differentiation ($v(D)$ constant). In Fig. 6b the fraction of stem cells is less than 10 % and the maximum self-renewal probability is kept small ($p_0 = 0.51$). For the special case of Hill functions it is shown in [39] that by keeping the maximum self-renewal probability p_0 very small it is possible to avoid oscillations while keeping the fraction of stem cells low. However, in agreement with the previous results this comes at the price of having a slow speed of regeneration indicated by the small value of p_0.

Figure 6c,d plot the trajectories for systems with feedback inhibition in both the self-renewal probability and the division rate of stem cells. Call $\beta(D) = 1 + hD^m$,

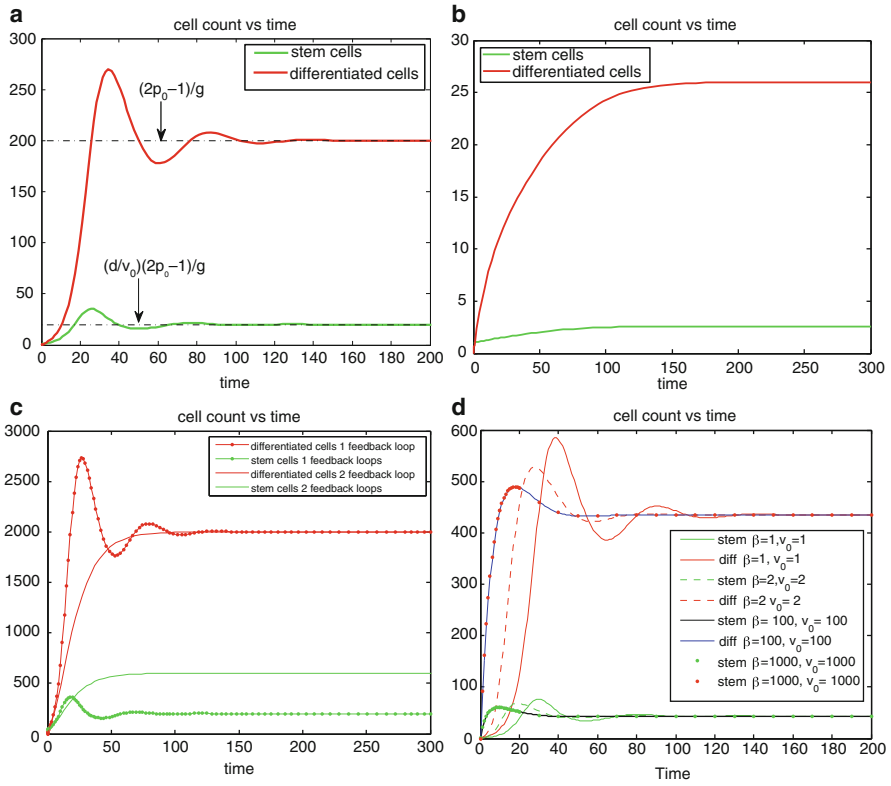

Fig. 6 (**a**) and (**b**) Cell population with one feedback loop. (**a**) The trajectories oscillate towards steady state values (*dotted line*). Parameters, $p_0 = 0.6$, $d = 0.1$, $g = 0.001$, $S(0) = 1$, $D(0) = 0$. (**b**) If there is only one feedback loop the maximum self-renewal probability must be very close to 0.5 to ensure that the trajectories approach the steady states monotonically. In this subfigure d and g are the same as in (**a**) but $p_0 = 0.513$. (**c**) and (**d**) cell population with two feedback loops. (**c**) The steady state number of differentiated cells depends only p_0 and g and is independent of feedback on the division rates. The steady state number of stem cells increases when the number of feedback loops increase from one to two. The addition of feedback in the division rate dampens or altogether eliminates the oscillations. (**d**) Fitting fixed steady state values of stem cells and differentiated cells values with different levels of feedback inhibition in the division rate. The stronger the feedback signal in the division rate the smoother the transition the equilibrium transition to equilibrium

then $v(D) = v_0/\beta(D)$ and $\beta(D)$ controls the strength of the inhibition signal. We can get a specific target division rate at equilibrium $\hat{v}$ with different combinations of the pair $(v_0, \beta(\hat{D}))$; the larger themagnitude of these quantities, the stronger the feedback in the division rate will be. Figure 6d plots the trajectories for the same target number of cells with different combinations of the pair $(v_0, \beta(\hat{D}))$. Note how the addition of feedback on the division rate provides for smoother and faster recoveries after a perturbation.

8 Tissue Regulation in a Spatial-Stochastic Model

We now want to assess the dynamics of tissue regulation in the spatial-stochastic model that was introduced earlier. In general we find that the addition of a spatial structure results in smoother transitions from perturbed states to equilibrium. When there are oscillations in the spatial model the amplitudes are smaller than those found in the corresponding mass action formulation (Fig. 7a,b). Moreover, as we discuss in [39] oscillation in the mass action model after extreme perturbation could result in the stochastic extinction of the stem cell pool. The number of these extinctions is greatly reduced by the addition of the spatial structure. For example, with the set of parameters ($p_0 = 0.7, v_0 = 0.2, g = 2 \times 10^{-5}, \beta = 1, d = 0.0025$), a perturbation of the initial conditions $(S(0), D(0)) = 0.1(\hat{S}, \hat{D})$ resulted in the stochastic extinction of the cell population in all of 100 independent simulations using the a stochastic version of the mass action model. By comparison extinction never took place in 30 simulations using the spatial-stochastic model with the same set of parameters and initial conditions.

In the spatial model we can divide stem cells into two categories: free stem cells, which have adjacent free lattice points and are thus capable of cell division; and trapped stem cells, which are completely surrounded by cells and are thus unable to divide. The equilibrium fraction of stem cells in the mass action model is the same as the equilibrium number of free stem cells in the spatial model. Hence, for the same set of parameters the equilibrium number of stem cells will be greater in the spatial model than in the non-spatial model (Fig. 7b,c).

Suppose that we start with a perturbation in which the number of differentiated cells is less than $\hat{D}$. Then the probability of differentiation is small and most cell divisions result in the production of two stem cells. Once the number of differentiated cells is above $\hat{D}$, differentiation becomes the more likely event and in the ODE model one sees a steep reduction in the number of stem cells. In the spatial model, however, the rapid growth phase means that the fraction of free stem cells is reduced as most stem cells become trapped by other stem cells. Only these free stem cells are able to divide, slowing down the speed at which they are depleted and thus reducing the severity of the oscillations. This behavior is exemplified by Fig. 7b.

9 Discussion

A wealth of data indicates that feedback loops play a central role in the regulation of healthy tissue. Recent data also supports the notion that tumors retain some of the architectural aspects of the underlying healthy tissue. It is thought that tumors are maintained and driven by so-called tumor stem cells or tumor initiating cells, and that the bulk of the tumor is made up of more differentiated cells that have a reduced ability to divide and therefore cannot maintain or initiate a cancer. In the light of

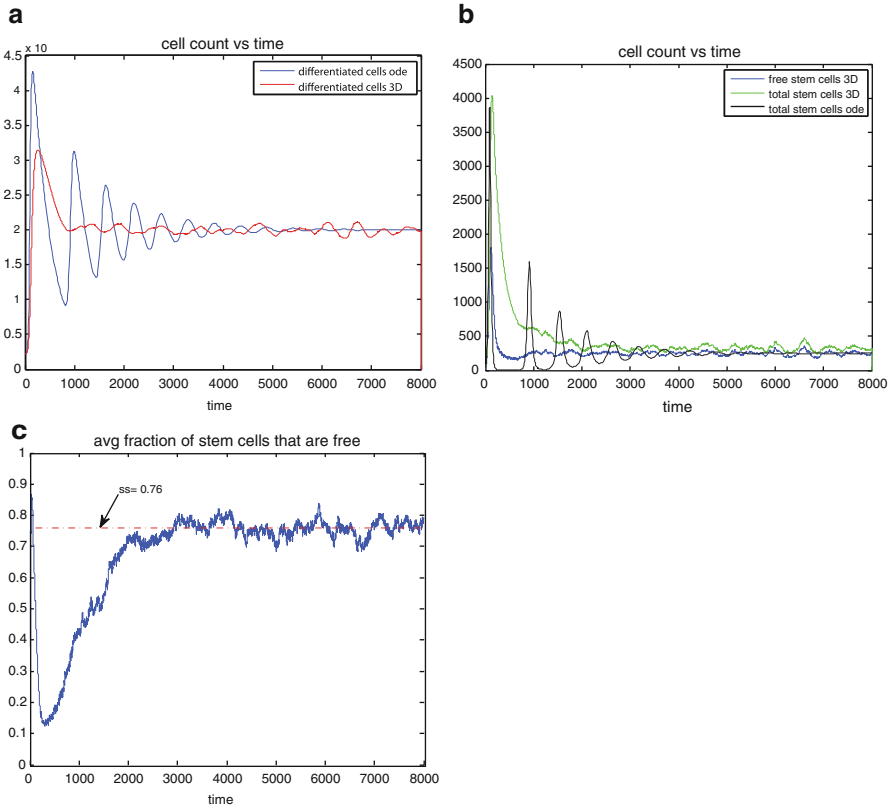

Fig. 7 (**a**) Cell count of differentiated cells vs time. The *blue line* was computed using the ODE model. The *red line* is the expected cell count in the spatial-stochastic model. (**b**) Cell count of stem cells. Results from the ODE (*black*) and expected cell count in spatial model (*green*). The expected number of cells in the spatial model is shown in *blue*. (**c**) Expected fraction of stem cells that are free in the three-dimensional model. Parameters in all figures are: $p_0 = 0.7$, $v_0 = 0.2$, $g = 2 \times 10^{-5}$, $\beta = 1$ and $d = 0.0025$

this, it is reasonable to assume that tumor initiation requires the loss of some of these feedback loops. In particular, two types of feedback mechanisms appear to be a common theme across different tissues: negative feedback on the rate of stem cell division, and negative feedback on the probability that a stem cell division results in self-renewal rather than in differentiation. Mutations can occur that lead to the loss of feedback signals produced by cells or that lead to a loss of response to the feedback signals by stem cells. Using an evolutionary dynamics model, it is found that only one sequence of events can lead to full escape from feedback control: The first step is loss of the cells' ability to respond to the differentiation feedback. While this leads to unbounded cell growth, the cell population grows relatively slowly because the emerging tumor is still regulated in part by remnants of the feedback system (inhibited growth). To escape this remaining regulation, cells also have to

lose the ability to respond to the division feedback control factors, leading to fast, uninhibited growth. We note that the order of events is crucial here. In a healthy cell population, mutant cells that do not respond to the division feedback will not enjoy a selective advantage and are therefore unlikely to emerge. Such mutants are only selected for and can only emerge in a background population that has already lost the ability to respond to the differentiation feedback factors.

Our analysis is supported by key mutations in carcinogenesis that disrupt negative feedback regulation of cell division patterns. For example, the protein transforming growth factor beta (TGF-β) plays a key role in tissue homeostasis by inhibiting mitosis and promoting cell differentiation [57]. Mutations that affect TGF-β receptors occur in gastric, biliary, pulmonary, ovarian, esophageal, and head and neck carcinomas [32]. Moreover, half of all pancreatic carcinomas and more than a quarter of colon cancers carry mutations that make cells irresponsive to TGF-β signals that inhibit cell division and promote differentiation [43, 59]. Another example comes from the epigenetic silencing of BMP4 receptors in glioblastomas [27]. BMP4 induces glia stem cells to differentiate, inhibiting cell proliferation [28].

Another line of evidence that supports the importance of the Sdiff- phenotype comes from the manipulation of the MYC gene. A mouse model of human hepatocellular carcinoma was developed, in which it is possible to regulate the expression of the human MYC oncogene in murine liver cells, suppressing it through doxycycline treatment [16,44,45]. Mice treated with doxycycline remained disease free, while those with active MYC developed malignant tumors that were locally invasive and able to metastasize. When MYC was subsequently inactivated, rapid tumor regression was observed that was associated with terminal differentiation into normal liver cells. MYC expression influences self-renewal and differentiation of cells, and thus influences the function $p(D)$ in our model. Activation of MYC corresponds to a corrupted differentiation feedback (i.e., to the Sdiff- phenotype in the model), whereas inhibition of MYC reverses this phenotype. The model predicts Sdiff- to be the initial event leading to uncontrolled growth. Even if cells have acquired other mutations that can also contribute to tumor progression, these mutations are predicted to promote growth only in cells that already have corrupted differentiation feedback. Hence, the model predicts that the restoration of the differentiation feedback loop, even in cells with further alterations, results in tumor regression. This same behavior is observed in the experiments where the macroscopic and malignant nature of the tumors indicate the presence of additional mutations, which are incapable of promoting growth in the absence of MYC [16, 44, 45].

Overall, these processes can give rise to five different categories of tumor growth laws, which we call “exponential,” “surface,” “sigmoidal,” “atypical,” and “multi-step.” Following an extensive literature search for different tumor growth patterns, we suggest that most can be assigned to one of these categories. Fitting our model to experimental data on in vitro and in vivo tumor cell growth, we demonstrated that the predicted growth patterns describe biological data well. The finding of inhibited tumor growth patterns in the literature is of particular interest. Such a growth pattern can only come about if the growing tumor is still partially subject to regulation

that has remained from the underlying tissue. This gives support to the notion that tumors are organized and structured according to similar principles as healthy tissue, at least early in the disease process. The finding of sub-cubic growth laws among data is particularly notable in this respect because it has not been possible to ascribe such slow growth to factors other than feedback. While we have shown that our model can describe a range of tumor growth data well, a crucial experimental test would be to document the presence of negative feedback loops in early tumors that are characterized by an inhibited growth pattern, and to further demonstrate that elimination of this feedback loop leads to accelerated tumor growth.

The findings discussed here have implications for elucidating carcinogenesis pathways in specific cancers. While we have identified the sequence of two key phenotypic events in the emergence of stem-cell-driven tumors, this does not mean that each event corresponds to a single mutation. The inactivation of feedback responses can involve a multi-step accumulation of mutations, the nature of which are most likely tissue specific. Hence, it will be important to identify the relevant feedback loops in the tissues under consideration, and to study the nature of the mutations that are required for the sequential escape documented here. This could lead to the discovery of new targets for therapeutic intervention.

We also discussed how the two feedback mechanisms affect the dynamics of tissue regulation. Feedback on the rate of stem cell differentiation uniquely determines the equilibrium number of differentiated cells and is by itself capable of maintaining tissue homeostasis. Feedback on rate of stem cell division controls the fraction of stem cells in the population and promotes faster recoveries from perturbations.

It was also found that when the system is recovering from a perturbation oscillations in the number of cells might take place, a behavior that may be dangerous and of no obvious biological value. Near equilibrium oscillations are more likely to occur when the steady state fraction of stem cells is small. Adding feedback inhibition on the division rate significantly dampens the magnitude of the oscillations and increases the speed at which the trajectories reach the steady states; the stronger the feedback signal the stronger the effect. Thus, even if feedback on the division rate is unnecessary to establish control, it promotes faster and more stable recoveries after an injury. The addition of spatial structure to the tissue also adds to the robustness of the systems, by eliminating oscillations or significantly reducing their amplitude.

Understanding the population dynamics that take place during tissue regeneration has important applications and has led to significants insights (see, e.g., [26]). In particular the study of oscillatory behavior is relevant to the dynamics of blood cells. Damped oscillations have been observed in healthy hematopoiesis [31]. Amongst pathologies periodic oscillations are a characteristic feature of cyclical neutropenia [6]. Furthermore, oscillatory behavior has also been identified in chronic and acute myeloid leukemia [1, 3, 12].

Two principal aims of regulatory mechanisms in hierarchical tissues are the maintenance of homeostasis, which prevents the onset of cancer, and the promotion of fast and reliable recovery from injuries. In this chapter we discussed several

mathematical models that identify key features of the regulatory mechanisms that promote tissue regeneration and stability. Furthermore, we discussed the phenotypical pathways by which cancer can escape tissue regulation and how this might leas to different types of tumor growth patterns. These insights could help the search for mutations that drive specific cancers and could lead to novel ideas for treatment.

Acknowledgements This work was funded by NIH grant R01 CA129286.

References

1. Adimy, M., Crauste, F., Ruan, S.: Modelling hematopoiesis mediated by growth factors with applications to periodic hematological diseases. Bull. Math. Biol. **68**, 2321–2351 (2006)
2. Alon, U.: An introduction to systems biology: design principles of biological circuits. Chapman and Hall/CRC mathematical and computational biology series, vol. 10. Chapman and Hall/CRC, Boca Raton (2007)
3. Andersen, L.K., Mackey, M.C.: Resonance in periodic chemotherapy: a case study of acute myelogenous leukemia. J. Theor. Biol. **209**, 113–130 (2001)
4. Arino, O., Kimmel, M.: Stability analysis of models of cell production systems. Math. Model. **7**(9), 1269–1300 (1986)
5. Ashkenazi, R., Gentry, S.N., Jackson, T.L.: Pathways to tumorigenesis–modeling mutation acquisition in stem cells and their progeny. Neoplasia **10**, 1170–1182 (2008)
6. Bernard, S., Bélair, J., Mackey, M.C.: Oscillations in cyclical neutropenia: new evidence based on mathematical modeling. J. Theor. Biol. **223**, 283–298 (2003)
7. Bocharov, G., Quiel, J., Luzyanina, T., Alon, H., Chiglintsev, E., Chereshnev, V., Meier-Schellersheim, M., Paul, W.E., Grossman, Z.: Feedback regulation of proliferation vs. differentiation rates explains the dependence of cd4 t-cell expansion on precursor number. Proc. Natl. Acad. Sci. USA **108**, 3318–3323 (2011)
8. Bru, A., Albertos, S., Subiza, J. Garcia-Asenjo, J., Bru, I.: The universal dynamics of tumor growth. Biophys. J. **85**, 2948–2961 (2003)
9. Choe, S.C., Zhao, G., Zhao, Z., Rosenblatt, J.D., Cho, H.-M., Shin, S.-U., Johnson, N.F.: Model for in vivo progression of tumors based on co-evolving cell population and vasculature. Sci. Rep. **1**, 31 (2011)
10. Chou, C.-S., Lo, W.-C., Gokoffski, K.K., Zhang, Y.-T., Wan, F.Y.M., Lander, A.D., Calof, A.L., Nie, Q.: Spatial dynamics of multistage cell lineages in tissue stratification. Biophys J. **99**, 3145–3154 (2010)
11. Clevers, H.: The cancer stem cell: premises, promises and challenges. Nat. Med. **17**, 313–319 (2011)
12. Colijn, C., Mackey, M.C.: A mathematical model of hematopoiesis–i. periodic chronic myelogenous leukemia. J. Theor. Biol. **237**, 117–132 (2005)
13. Daluiski, A., Engstrand, T., Bahamonde, M.E., Gamer, L.W., Agius, E., Stevenson, S.L., Cox, K., Rosen, V., Lyons, K.M.: Bone morphogenetic protein-3 is a negative regulator of bone density. Nat. Genet. **27**, 84–88 (2001)
14. Elgjo, K., Reichelt, K.L.: Chalones: from aqueous extracts to oligopeptides. Cell Cycle **3**, 1208–1211 (2004)
15. Enderling, H., Anderson, A.R.A., Chaplain, M.A.J., Beheshti, A., Hlatky, L., Hahnfeldt, P.: Paradoxical dependencies of tumor dormancy and progression on basic cell kinetics. Cancer Res. **69** 8814–8821 (2009)

16. Felsher, D.W.: Cancer revoked: oncogenes as therapeutic targets. Nat. Rev. Cancer **3**, 375–380 (2003)
17. Frank, S.A., Dynamics of Cancer: Incidence, Inheritance, and Evolution. Princeton University Press, Princeton (2007)
18. Freyer, J.P., Sutherland, R.M.: A reduction in the in situ rates of oxygen and glucose consumption of cells in emt6/ro spheroids during growth. J. Cell Physiol. **124**, 516–524 (1985)
19. Freyer, J.P., Sutherland, R.M.: Regulation of growth saturation and development of necrosis in emt6/ro multicellular spheroids by the glucose and oxygen supply. Cancer Res. **46**, 3504–3512 (1986)
20. Gillespie, D.T.: Exact stochastic simulation of coupled chemical reactions. J. Phys. Chem. **81**(25), 2340–2361 (1977)
21. Guiot, C., Degiorgis, P.G., Delsanto, P.P., Gabriele, P., Deisboeck, T.S.: Does tumor growth follow a universal law? J. Theor. Biol. **225**, 147–151 (2003)
22. Hart, D., Shochat, E., Agur, Z.: The growth law of primary breast cancer as inferred from mammography screening trials data. Br. J. Cancer **78**, 382–387 (1998)
23. Johnston, M.D., Edwards, C.M., Bodmer, W.F., Maini, P.K., Chapman, S.J.: Mathematical modeling of cell population dynamics in the colonic crypt and in colorectal cancer. Proc. Natl. Acad. Sci. USA **104**, 4008–4013 (2007)
24. Knighton, D., Ausprunk, D., Tapper, D., Folkman, J.: Avascular and vascular phases of tumour growth in the chick embryo. Br. J. Cancer **35**, 347–356 (1977)
25. Laird, A.K.: Dynamics of tumor growth. Br. J. Cancer **13**, 490–502 (1964)
26. Lander, A.D., Gokoffski, K.K., Wan, F.Y.M., Nie, Q., Calof, A.L.: Cell lineages and the logic of proliferative control. PLoS Biol. **7**, e15 (2009)
27. Lee, J., Son, M.J., Woolard, K., Donin, N.M., Li, A., Cheng, C.H., Kotliarova, S., Kotliarov, Walling, Y.J., Ahn, S., Kim, M., Totonchy, M., Cusack, T., Ene, C., Ma, H., Su, Q., Zenklusen, J.C., Zhang, W., Maric, D., Fine, H.A.: Epigenetic-mediated dysfunction of the bone morphogenetic protein pathway inhibits differentiation of glioblastoma-initiating cells. Cancer Cell **13**, 69–80 (2008)
28. Lim, D.A., Tramontin, A.D., Trevejo, J.M., Herrera, D.G., García-Verdugo, J.M., Alvarez-Buylla, A.: Noggin antagonizes bmp signaling to create a niche for adult neurogenesis. Neuron **28**, 713–726 (2000)
29. Mandonnet, E., Delattre, J.-Y., Tanguy, M.-L., Swanson, K.R., Carpentier, A.F., Duffau, H., Cornu, P., Van Effenterre, R., Alvord, Jr. E.C., Capelle, L.: Continuous growth of mean tumor diameter in a subset of grade ii gliomas. Ann. Neurol. **53**, 524–528 (2003)
30. Marciniak-Czochra, A., Stiehl, T., Ho, A.D., Jäger, W., Wagner, W.: Modeling of asymmetric cell division in hematopoietic stem cells–regulation of self-renewal is essential for efficient repopulation. Stem Cells Dev. **18**, 377–385 (2009)
31. Marciniak-Czochra, A., Stiehl, T.: Model based parameter estimation: theory and applications. Contributions in mathematical and computational sciences. Mathematical Models of Hematopoietic Reconstitution after Stem Cell Transplantation, vol. 4, pp. 191–207. Springer, New York (2013)
32. Massagué, J.: Tgf? in cancer. Cell **103**, 295–309 (2000)
33. McPherron, A.C., Lawler, A.M., Lee, S.J.: Regulation of skeletal muscle mass in mice by a new tgf-beta superfamily member. Nature **387**, 83–90 (1997)
34. Meza, R., Jeon, J., Moolgavkar, S.H., Luebeck, E.G.: Age-specific incidence of cancer: Phases, transitions, and biological implications. Proc. Natl. Acad. Sci. USA **105**, 16284–16289 (2008)
35. Moolgavkar, S.H., Knudson, Jr. A.G.: Mutation and cancer: a model for human carcinogenesis. J. Natl. Cancer Inst. **66**, 1037–1052 (1981)
36. Retsky, M.W., Swartzendruber, D.E., Wardwell, R.H., Bame, P.D.: Is gompertzian or exponential kinetics a valid description of individual human cancer growth? Med. Hypotheses **33**, 95–106 (1990)

37. Reuss, R., Ludwig, J., Shirakashi, R., Ehrhart, F., Zimmermann, H., Schneider, S., Weber, M.M., Zimmermann, U., Schneider, H., Sukhorukov, V.L.: Intracellular delivery of carbohydrates into mammalian cells through swelling-activated pathways. J. Membr. Biol. **200**, 67–81 (2004)
38. Rodriguez-Brenes, I.A., Komarova, N.L., Wodarz, D.: Evolutionary dynamics of feedback escape and the development of stem-cell-driven cancers. Proc. Natl. Acad. Sci. USA **108**, 18983–18988 (2011)
39. Rodriguez-Brenes, I.A., Wodarz, D., Komarova, N.L.: Stem cell control, oscillations, and tissue regeneration in spatial and non-spatial models. Front Oncol. **3**, 82 (2013)
40. Rodriguez-Brenes, I.A., Komarova, N.L., Wodarz, D.: Tumor growth dynamics: insights into evolutionary processes. Trends Ecol. Evol. **28**, 597–604 (2013)
41. Rodriguez-Brenes, I.A., Wodarz, D., Komarova, N.L.: Minimizing the risk of cancer: tissue architecture and cellular replication limits. J. R. Soc. Interface **10**, 20130410 (2013)
42. Rodriguez-Brenes, I.A., Komarova, N.L., Wodarz, D.: Cancer-associated mutations in healthy individuals: assessing the risk of carcinogenesis. Cancer Res. **74**(6), 1661–1669 (2014)
43. Rozenblum, E., Schutte, M., Goggins, M., Hahn, S.A., Panzer, S., Zahurak, M., Goodman, S.N., Sohn, T.A., Hruban, R.H., Yeo, C.J., Kern, S.E.: Tumor-suppressive pathways in pancreatic carcinoma. Cancer Res. **57**, 1731–1734 (1997)
44. Shachaf, C.M., Kopelman, A.M., Arvanitis, C., Karlsson, A., Beer, S., Mandl, S., Bachmann, M.H., Borowsky, A.D., Ruebner, B., Cardiff, R.D., Yang, Q., Bishop, J.M., Contag, C.H., Felsher, D.W.: Myc inactivation uncovers pluripotent differentiation and tumour dormancy in hepatocellular cancer. Nature **431**, 1112–1117 (2004)
45. Shachaf, C.M., Felsher, D.W.: Tumor dormancy and myc inactivation: pushing cancer to the brink of normalcy. Cancer Res. **65**, 4471–4474 (2005)
46. Shackney, S.E.: A computer model for tumor growth and chemotherapy, and its application to l1210 leukemia treated with cytosine arabinoside (nsc-63878). Cancer Chemother. Rep. **54**, 399–429 (1970)
47. Shizuru, J.A., Negrin, R.S., Weissman, I.L.: Hematopoietic stem and progenitor cells: clinical and preclinical regeneration of the hematolymphoid system. Annu. Rev. Med. **56**, 509–538 (2005)
48. Simeoni, M., Magni, P., Cammia, C., De Nicolao, G., Croci, V., Pesenti, E., Germani, M., Poggesi, I., Rocchetti, M.: Predictive pharmacokinetic-pharmacodynamic modeling of tumor growth kinetics in xenograft models after administration of anticancer agents. Cancer Res. **64**, 1094–1101 (2004)
49. Simpson-Herren, L., Lloyd, H.H.: Kinetic parameters and growth curves for experimental tumor systems. Cancer Chemother. Rep. **54**,143–174 (1970)
50. Skipper, H.E., Schabel, Jr. F.M., Wilcox, W.S.: Experimental evaluation of potential anticancer agents. xiii. on the criteria and kinetics associated with curability of experimental leukemia. Cancer Chemother. Rep. **35**, 1–111 (1964)
51. Spratt, J.A., von Fournier, D., Spratt, J.S., Weber, E.E.: Decelerating growth and human breast cancer. Cancer **71**, 2013–2019 (1993)
52. Steel, G.G.: Growth Kinetics of Tumours: Cell Population Kinetics in Relation to the Growth and Treatment of Cancer. Clanesdon press, Oxford (1977)
53. Squartini, F.: Strain differences in growth on mouse mammary tumors. J. Nat. Cancer Inst. **26**, 81 (1961)
54. Tomlinson, I.P., Bodmer, W.F.: Failure of programmed cell death and differentiation as causes of tumors: some simple mathematical models. Proc. Natl. Acad. Sci. USA **92**, 11130–11134 (1995)
55. Tzeng, Y.-S., Li, H., Kang, Y.-L., Chen, W.-C., Cheng, W.-C., Lai, D.-M.: Loss of cxcl12/sdf-1 in adult mice decreases the quiescent state of hematopoietic stem/progenitor cells and alters the pattern of hematopoietic regeneration after myelosuppression. Blood **117**, 429–439 (2011)

56. Weedon-Fekjaer, H., Lindqvist, B.H., Vatten, L.J., Aalen, O.O., Tretli, S.: Breast cancer tumor growth estimated through mammography screening data. Breast Cancer Res. **10**(3), R41 (2008)
57. Weinberg, R.A.: The Biology of Cancer. Garland Science, New York (2007)
58. Werner, B., Dingli, D., Lenaerts, T., Pacheco, J.M., Traulsen, A.: Dynamics of mutant cells in hierarchical organized tissues. PLoS Comput. Biol. **7**, e1002290 (2011)
59. Woodford-Richens, K.L., Rowan, A.J., Gorman, P., Halford, S., Bicknell, D.C., Wasan, H.S., Roylance, R.R., Bodmer, W.F., Tomlinson, I.P.: Smad4 mutations in colorectal cancer probably occur before chromosomal instability, but after divergence of the microsatellite instability pathway. Proc. Natl. Acad. Sci. USA **98**, 9719–9723 (2001)
60. Wu, H.-H., Ivkovic, S., Murray, R.C., Jaramillo, S., Lyons, K.M., Johnson, J.E., Calof, A.L.: Autoregulation of neurogenesis by gdf11. Neuron **37**, 197–207 (2003)
61. Yamasaki, K., Toriu, N., Hanakawa, Y., Shirakata, Y., Sayama, K., Takayanagi, A., Ohtsubo, M., Gamou, S., Shimizu, N., Fujii, M., Miyazono, K., Hashimoto, K.: Keratinocyte growth inhibition by high-dose epidermal growth factor is mediated by transforming growth factor beta autoinduction: a negative feedback mechanism for keratinocyte growth. J. Invest. Dermatol. **120**, 1030–1037 (2003)
62. Zhang, L., Lander, A.D., Nie, Q.: A reaction-diffusion mechanism influences cell lineage progression as a basis for formation, regeneration, and stability of intestinal crypts. BMC Syst. Biol. **6**, 93 (2012)